CHIN. PHYS. LETT. Vol. 28, No. 7 (2011) 075205

# A Modified Third-Order Semi-Discrete Central-Upwind Scheme for MHD Simulation *

JI Zhen(纪珍)[1,2**], ZHOU Yu-Fen(周玉芬)[1], HOU Tian-Xiang(侯天相)[3]

[1] *State Key Laboratory of Space Weather, Center for Space Science and Applied Research, Chinese Academy of Sciences, Beijing 100190*
[2] *Graduate School, Chinese Academy of Sciences, Beijing 100049*
[3] *China Meteorological Administration Training Centre, Beijing 100081*

(Received 17 February 2011)

*The Kurganov scheme is a third-order semi-discrete central numerical algorithm. The high solution of the scheme is ensured by a piecewise quadratic non-oscillatory reconstruction which consists of the cell-average data. We employ a modification of the smooth limiter of reconstruction in a simple way. The modified limiter possesses rigorous positivity and the reformulation does not change the non-oscillatory property of reconstruction. In order to explore the potential capability of application of the modified Kurganov scheme to magnetohydrodynamics (MHD) and resistive magnetohydrodynamics (RMHD) equations, two numerical problems are simulated in two dimensions (2D). These numerical simulations demonstrate that the modified Kurganov scheme keeps high precision and has stable reliable results for MHD and RMHD applications.*

*PACS: 52.30.Cv, 95.30.Qd* DOI:10.1088/0256-307X/28/7/075205

The Kurganov method has been proposed in a series of papers.[1–5] This scheme is a high-order semi-discrete central Godunov-type method employing more precise information of the local speeds of waves. This central scheme has the advantages such as high solution, small numerical dissipation and simplicity. It also has no Riemann solvers and characteristic decomposition. In recent years, some researchers have applied the semi-discrete scheme into various problems with source terms and advanced the fourth- or fifth-order schemes by constructing different reconstructions.[6–11] In order to further reduce the numerical diffusion, Kurganov and his colleagues have developed the semi-discrete central scheme into semi-discrete central-upwind scheme.[2,12–14] The semi-discrete central-upwind schemes not only retain the advantages of central schemes but also are characterized by upwind nature, since the width of the Riemann fans is estimated by one-sided information of the local propagation speeds. There are three components of this method: a piecewise polynomial reconstruction, a spatial flux discretization and an ordinary differential solver. In order to obtain third-order accuracy, the essentially non-oscillatory (ENO)[15,16] reconstruction or its weighted extensions[17–19] are used to build a piecewise quadratic approximation. This kind of reconstruction is constructed by a quadratic polynomial interpolant function, a convex combination of the function and the given cell averages.

In two dimensions, the reconstruction is a bivariate quadratic polynomial. This reformulation may result in an oscillatory interpolant and a negative smooth limiter. To overcome this shortcoming, Kurganov *et al.*[1] has proposed another algorithm of smooth limiter at local extreme points. However, this smooth limiter can not always fill the requirement: $1-\theta = O(\Delta x^3)$ and in their paper, they have not proved that the reconstruction is non-oscillatory. In order to solve this problem, we redefine some correlation functions to obtain the corresponding smooth limiter and reconstruction polynomials in this Letter. It can be proved mathematically that the expression of smooth limiter is positive and the polynomials are non-oscillatory in all directions. We will briefly describe the Kurganov method and give a detailed introduction of the modified smooth limiter.

Consider the two-dimensional hyperbolic conservation laws

$$u_t + f(u)_x + g(u)_y = 0. \tag{1}$$

For the sake of simplicity, uniform grids are considered. Let $(x_j, y_k) = (j\Delta x, k\Delta y)$, $(x_{j\pm\frac{1}{2}}, y_{k\pm\frac{1}{2}}) = ((j\pm\frac{1}{2})\Delta x, (k\pm\frac{1}{2})\Delta y)$, $t^n = n\Delta t, u_j^n = u(x_j, t^n)$, with $\Delta x$, $\Delta y$, $\Delta t$ being the grid lengths and time step.

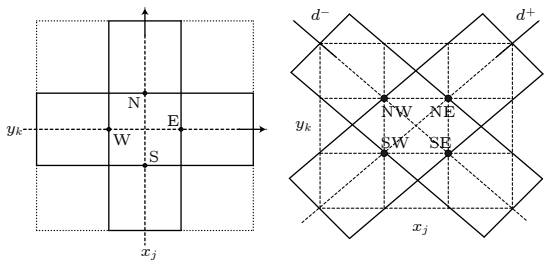


**Fig. 1.** (a) The corresponding points along the coordinates for $u$. (b) The points along the diagonal line.

According to Refs. [1,2], using the genuinely multi-dimensional approach, the corresponding semi-discrete central-upwind scheme for Eq. (1) is

$$\frac{d}{dt}\bar{u}_{j,k}(t) = -\frac{H^x_{j+\frac{1}{2},k}(t) - H^x_{j-\frac{1}{2},k}(t)}{\Delta x} - \frac{H^y_{j,k+\frac{1}{2}}(t) - H^y_{j,k-\frac{1}{2}}(t)}{\Delta y}, \tag{2}$$

*Supported by the National Natural Science Foundation of China under Grant Nos 40904050 and 40874077, and the Specialized Research Fund for State Key Laboratories.
**Email: zji@spaceweather.ac.cn
© 2011 Chinese Physical Society and IOP Publishing Ltd

where the numerical fluxes are

$$H^x_{j+\frac{1}{2},k} = \frac{a^+_{j+\frac{1}{2},k}}{6(a^+_{j+\frac{1}{2},k} - a^-_{j+\frac{1}{2},k})}\Big[f(u^{NE}_{j,k}) + 4f(u^E_{j,k}) + f(u^{SE}_{j,k})\Big] - \frac{a^-_{j+\frac{1}{2},k}}{6(a^+_{j+\frac{1}{2},k} - a^-_{j+\frac{1}{2},k})}\Big[f(u^{NW}_{j+1,k}) + 4f(u^W_{j+1,k}) + f(u^{SW}_{j+1,k})\Big] + \frac{a^+_{j+\frac{1}{2},k}a^-_{j+\frac{1}{2},k}}{6(a^+_{j+\frac{1}{2},k} - a^-_{j+\frac{1}{2},k})}\Big[u^{NW}_{j+1,k} - u^{NE}_{j,k} + 4(u^W_{j+1,k} - u^E_{j,k}) + u^{SW}_{j+1,k} - u^{SE}_{j,k}\Big],$$

$$H^y_{j+\frac{1}{2},k} = \frac{b^+_{j,k+\frac{1}{2}}}{6(b^+_{j,k+\frac{1}{2}} - b^-_{j,k+\frac{1}{2}})}\Big[g(u^{NW}_{j,k}) + 4g(u^N_{j,k}) + g(u^{NE}_{j,k})\Big] - \frac{b^-_{j,k+\frac{1}{2}}}{6(b^+_{j,k+\frac{1}{2}} - b^-_{j,k+\frac{1}{2}})}\Big[g(u^{SW}_{j,k+1}) + 4g(u^S_{j,k+1}) + g(u^{SE}_{j,k+1})\Big] + \frac{b^+_{j,k+\frac{1}{2}}b^-_{j,k+\frac{1}{2}}}{6(b^+_{j,k+\frac{1}{2}} - b^-_{j,k+\frac{1}{2}})}\Big[u^{SW}_{j,k+1} - u^{NW}_{j,k} + 4(u^S_{j,k+1} - u^N_{j,k}) + u^{SE}_{j,k+1} - u^{NE}_{j,k}\Big].$$

Here the one-sided local speeds $a^{\pm}_{j+\frac{1}{2},k}$, $b^{\pm}_{j,k+\frac{1}{2}}$ and the corresponding point values $u_{j,k}$ are the ones described in Ref. [2] (see Fig. 1). The notation

$$\bar{u}_{j,k} = \frac{1}{\Delta x \Delta y}\iint_{C_{j,k}} p^n_{j,k}(x,y)dxdy$$

is the cell average over the interval $C_{j,k} = [x_{j-\frac{1}{2}}, x_{j+\frac{1}{2}}] \times [y_{k-\frac{1}{2}}, y_{k+\frac{1}{2}}]$. The quadratic polynomials $p^n_{j,k}$ are convex combination of the basic parabolas $q^n_{j,k}$ and the piecewise linear interpolant $L^n_{j,k}$. The expression of $p^n_{j,k}$ is

$$p^n_{j,k} = (1-\theta^n_{j,k})L^n_{j,k} + \theta^n_{j,k}\ q^n_{j,k}, 0 \leqslant \theta^n_{j,k} \leqslant 1, \quad (3)$$

where $\theta^n_{j,k}$ is a smooth limiter.

In the following, we will describe the redefined piecewise parabolic reconstruction in detail. In one dimension, the algebraic polynomials $q^n_j$ is

$$q^n_j(x) = \bar{u}^n_j - \frac{1}{24}(\bar{u}^n_{j+1} - 2\bar{u}^n_j + \bar{u}^n_{j-1}) + \frac{1}{2}(\bar{u}^n_{j+1} - \bar{u}^n_{j-1})\frac{(x-x_j)}{\Delta x} + \frac{1}{2}(\bar{u}^n_{j+1} - 2\bar{u}^n_j + \bar{u}^n_{j-1})\frac{(x-x_j)^2}{(\Delta x)^2}. \quad (4)$$

We generalize this idea for the 2D case. For the points along the line $y \equiv y_k$, $q^n_{j,k}$ have the form

$$q^n_{j,k}(x,y_k) = \bar{u}^n_j - \frac{1}{24}(\bar{u}^n_{j+1} - 2\bar{u}^n_j + \bar{u}^n_{j-1}) - \frac{1}{24}(\bar{u}^n_{j,k+1} - 2\bar{u}^n_{j,k} + \bar{u}^n_{j,k-1}) + \frac{1}{2}(\bar{u}^n_{j+1} - \bar{u}^n_{j-1})\frac{(x-x_j)}{\Delta x} + \frac{1}{2}(\bar{u}^n_{j+1} - 2\bar{u}^n_j + \bar{u}^n_{j-1})\frac{(x-x_j)^2}{(\Delta x)^2}. \quad (5)$$

Let $\Delta^{(j)}_k = \frac{1}{24}(\bar{u}^n_{j,k+1} - 2\bar{u}^n_{j,k} + \bar{u}^n_{j,k-1})$, one can derive the relationship $q^n_{j,k}(x,y_k) = q^n_j(x) - \Delta^{(j)}_k$. For the given $y_k$, we can substitute $q^n_{j,k}$ into the formulae

$$M_{j,k} = \max_{x\in I_j}\ q^n_{j,k}(x,y_k), \quad M_j = \max_{x\in I_j}\ q^n_j(x),$$
$$m_{j,k} = \min_{x\in I_j}\ q^n_{j,k}(x,y_k), \quad m_j = \min_{x\in I_j}\ q^n_j(x),$$

where $I_j$ is the cell $[x_{j-\frac{1}{2}}, x_{j+\frac{1}{2}}]$. Thus it is possible to deduce that $M^n_{j,k} = M^n_j - \Delta^{(j)}_k$, $m^n_{j,k} = m^n_j - \Delta^{(j)}_k$.

In terms of the above definition, we redefine the linear function $L^n_{j,k}$, the values of $M$, $m$ at $(x_{j\pm\frac{1}{2}}, y_k)$ and the limiter $\theta^n_{j,k}$,

$$L^n_{j,k}(x_j,y_k) = \bar{u}^n_{j,k} + s^n_{j,k}(x-x_j),$$
$$s^n_{j,k} = \text{minmod}\left\{\frac{(\bar{u}^n_{j+1,k} - \bar{u}^n_{j,k})}{\Delta x}, \frac{(\bar{u}^n_{j,k} - \bar{u}^n_{j-1,k})}{\Delta x}\right\}, \quad (6)$$

$$M^n_{j\pm\frac{1}{2},k} = \max\left\{\frac{1}{2}\Big(L^n_j\big(x_{j\pm\frac{1}{2}}\big) + L^n_{j\pm1}\big(x_{j\pm\frac{1}{2}}\big)\Big) - \Delta^{(j\pm1)}_k, q^n_{j\pm1,k}\big(x_{j\pm\frac{1}{2}}, y_k\big)\right\},$$
$$m^n_{j\pm\frac{1}{2},k} = \min\left\{\frac{1}{2}\Big(L^n_j\big(x_{j\pm\frac{1}{2}}\big) + L^n_{j\pm1}\big(x_{j\pm\frac{1}{2}}\big)\Big) - \Delta^{(j\pm1)}_k, q^n_{j\pm1,k}\big(x_{j\pm\frac{1}{2}}, y_k\big)\right\}, \quad (7)$$

$$\theta^n_{j,k} = \begin{cases} \min\left\{\frac{M^n_{j+\frac{1}{2},k} - L^n_{j,k}\left(x_{j+\frac{1}{2}}\right) + \Delta^{(j+1)}_k}{M^n_{j,k} - L^n_{j,k}\left(x_{j+\frac{1}{2}}\right) + \Delta^{(j)}_k}, \frac{m^n_{j-\frac{1}{2},k} - L^n_{j,k}\left(x_{j-\frac{1}{2}}\right) + \Delta^{(j-1)}_k}{m^n_{j,k} - L^n_{j,k}\left(x_{j-\frac{1}{2}}\right) + \Delta^{(j)}_k}, 1\right\}, & \bar{u}^n_{j-1} < \bar{u}^n_j < \bar{u}^n_{j+1}, \\ \min\left\{\frac{M^n_{j-\frac{1}{2},k} - L^n_{j,k}\left(x_{j-\frac{1}{2}}\right) + \Delta^{(j-1)}_k}{M^n_{j,k} - L^n_{j,k}\left(x_{j-\frac{1}{2}}\right) + \Delta^{(j)}_k}, \frac{m^n_{j+\frac{1}{2},k} - L^n_{j,k}\left(x_{j+\frac{1}{2}}\right) + \Delta^{(j+1)}_k}{m^n_{j,k} - L^n_{j,k}\left(x_{j+\frac{1}{2}}\right) + \Delta^{(j)}_k}, 1\right\}, & \bar{u}^n_{j-1} > \bar{u}^n_j > \bar{u}^n_{j+1}, \\ 1, & \text{else.} \end{cases}$$

Substituting $q^n_{j,k}$ into Eq. (7) yields

$$M^n_{j\pm\frac{1}{2},k} = M^n_{j\pm\frac{1}{2}} - \Delta^{(j\pm1)}_k, \quad m^n_{j\pm\frac{1}{2},k} = m^n_{j\pm\frac{1}{2}} - \Delta^{(j\pm1)}_k.$$

According to these definitions, the limiter can be simplified to

$$\theta^n_{j,k} = \begin{cases} \min\left\{\frac{M^n_{j+\frac{1}{2}} - L^n_{j,k}\left(x_{j+\frac{1}{2}}\right)}{M^n_j - L^n_{j,k}\left(x_{j+\frac{1}{2}}\right)}, \frac{m^n_{j-\frac{1}{2}} - L^n_{j,k}\left(x_{j-\frac{1}{2}}\right)}{m^n_j - L^n_{j,k}\left(x_{j-\frac{1}{2}}\right)}, 1\right\}, & \bar{u}^n_{j-1} < \bar{u}^n_j < \bar{u}^n_{j+1}, \\ \min\left\{\frac{M^n_{j-\frac{1}{2}} - L^n_{j,k}\left(x_{j-\frac{1}{2}}\right)}{M^n_j - L^n_{j,k}\left(x_{j-\frac{1}{2}}\right)}, \frac{m^n_{j+\frac{1}{2}} - L^n_{j,k}\left(x_{j+\frac{1}{2}}\right)}{m^n_j - L^n_{j,k}\left(x_{j+\frac{1}{2}}\right)}, 1\right\}, & \bar{u}^n_{j-1} > \bar{u}^n_j > \bar{u}^n_{j+1}, \\ 1, & \text{else.} \end{cases} \tag{8}$$

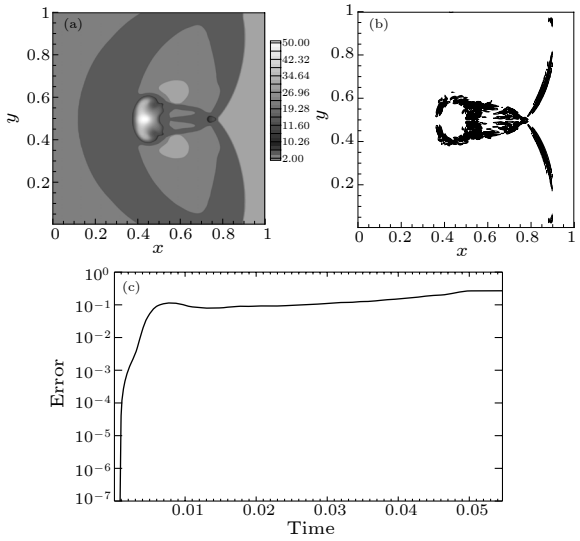


**Fig. 2.** (a) Density contours of interaction between shock and plasma cloud at $t = 0.06$ using a $200 \times 200$ uniform grid; (b) $\nabla \cdot \boldsymbol{B}$ contours at $t = 0.06$ using a $200 \times 200$ uniform grid; (c) the evolution of the error.

The combination of Eqs. (2)–(6) and Eq. (8) is the modified third-order semi-discrete central-upwind method. Different from Eq. (3.25) and Eq. (3.26) defined by Kurganov *et al.*[1] the definitions of $L^n_{j,k}$ and $s^n_{j,k}$ are employed in Eq. (6). Moreover, the definition of $q^n_{j,k}$ in 2D is modified in Eq. (5), which is different from Eq. (3.24) defined by Kurganov *et al.*[1] The difference between our modification and the former expression lies in that the modified $q^n_{j,k}$ goes without the term $\Delta^{(j)}_k$. Thus, the modified smooth limiter is greatly simplified. Through exact mathematical demonstration, it can be proved that the reconstruction is non-oscillatory in all directions. The mathematical proof is omitted here for save of space.

For verifying the application of the modified scheme in MHD and RMHD, here two numerical simulations are discussed in 2D. The third order Runge–Kutta time discrete method is used in all the simulations to keep the stability of the method. The first test is interaction between a magnetosonic shock and a denser cloud. This problem has been widely considered in the literature[20–22] to model the disruption of a high density cloud by a strong shock wave. The computation domain is $[0, 1] \times [0, 1]$. The initial conditions are

$$(\rho,\ u_1,\ u_2,\ u_3,\ p,\ B_1,\ B_2,\ B_3) = \begin{cases} (3.86859,\ 11.2536,\ 0,\ 0,\ 167.345,\ 0,\ 2.1826182,\ -2.1826182), & x < 0.05, \\ (1,\ 0,\ 0,\ 0,\ 1,\ 0,\ 0.56418985,\ 0.56418985), & x > 0.05, \end{cases}$$

and $\gamma = 5/3$. Thus, a discontinuity parallel to the $y$ axis at $x = 0.05$. There is a circular cloud which is centered at $(0.25, 0.5)$ with a high density $\rho = 10$ and radius $r = 0.15$. The cloud is in the magneto-hydrostatic balance with the surrounding fluid. The open boundary condition is used for all boundaries of the computation domain.

Figure 2(a) is contour plots of the density for $200 \times 200$ at $t = 0.06$. The Courant–Friedrichs–Lewy (CFL) number is 0.6. The profile is almost the same as those obtained by Han and Tang.[21] The density contours show that the modified scheme can catch shocks accurately. Figure 2(b) is the divergence contours of magnetic field at $t = 0.06$. The distribution of $\nabla \cdot \boldsymbol{B}$ displays that the divergence of magnetic field is concentrated around the denser cloud and the main shock. Figure 2(c) expresses the evolution of the error along with time, in which the error $\sigma = \frac{\sum |\nabla \cdot \boldsymbol{B}|}{nx \times ny}$ (the denominator is the total number of simulation nodes). Here $\nabla \cdot \boldsymbol{B} = \frac{\partial B}{\partial x} + \frac{\partial B}{\partial y}$, in which $\frac{\partial B}{\partial x}$ and $\frac{\partial B}{\partial y}$ are calculated by the central difference method. The figure shows that the error is not accumulated perniciously along with time, which means that the modified scheme is suitable and stable for solving MHD problems.

The second experiment is magnetic reconnection. Here the investigation is taken for the turbulent magnetic reconnections near a local current sheet by the RMHD models. The same problem solved by Wei *et al.*[23,24] is chosen for simulation. This numerical study is used to simulate the magnetic reconnection phenomena in interplanetary space. The computational domain is $[-3, 3] \times [-3, 3]$. The two plasma bulks with the same momentum and radius ($r = 0.3$) are located on the sides of the current sheet and centered at $(-1.5, 1.5)$ and $(1.5, -1.5)$, respectively. Their initial values are given as follows: $\rho_{M1} = 3.8\rho_\infty$, $V_{M1} = -1.036V_{A0}i_y$, $\rho_{M2} = 2.0\rho_\infty$, $V_{M2} = 1.912V_{A0}i_y$. The assumptions of the current

sheet are $B_0(y) = b_{x0}b_{z0}\tanh(y)i_x + b_{z0}i_z$, $\rho_0(y) = \rho_\infty + \frac{b_{x0}^2 b_{z0}^2}{8\pi RT_0}\mathrm{sech}^2(y)$, $V = 0$ and $b_{x0} = 0.1, b_{z0} = b_\infty$. The open boundaries are employed at $y = \pm 3$ and the periodic boundaries are taken at $x = \pm 3$. The typical interplanetary solar wind parameters $b_\infty = 8.33\,\mathrm{nT}$, $N_0 = 5\mathrm{proton/cm}^3$, $T_0 = 1. \times 10^5\,\mathrm{K}$, $V_{A0} = \frac{B_\infty}{(4\pi\rho_\infty)^{1/2}}$ are used as the dimensionless parameters. $R$ is the gas constant.

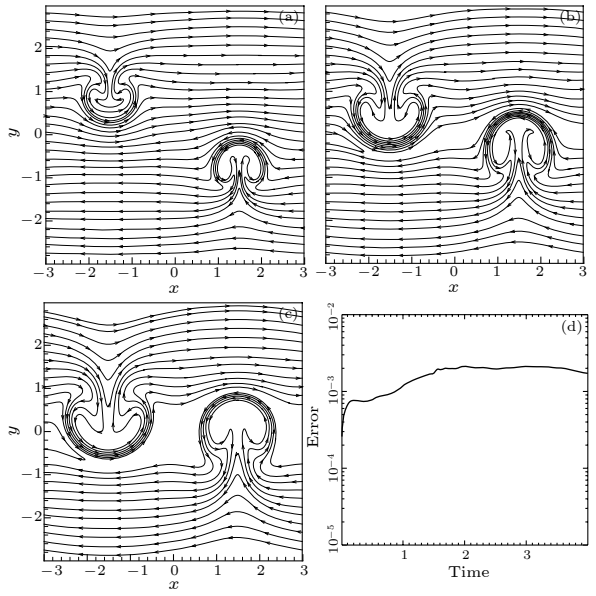


**Fig. 3.** Time evolution of the magnetic field lines in the $x$–$y$ plane for magnetic reconnection: (a) $t = 2\tau_A$, (b) $t = 4\tau_A$, (c) $t = 6\tau_A$, (d) the evolution of the error at $t = 4\tau_A$.

Figures 3(a), 3(b) and 3(c) show the temporal evolution of magnetic field lines with CFL of 0.1 for uniform grids $200 \times 200$ at $t = 2\tau_A$, $t = 4\tau_A$, $t = 6\tau_A$, respectively. The results are almost the same as those obtained by Wei *et al.*[24] Under the same momentum, the occurrence of magnetic reconnection and the distortion of magnetic field lines begin earlier for the high speed plasma bulk than the high density plasma bulk. The results indicate that the modified method can catch the magnetic reconnection preferably. Figure 3(d) shows the evolution of the error along with time. The error of divergence of magnetic field is under $10^{-2}$ for most parts of time. Thus, the modified algorithm keeps the properties of high-order scheme with a small CFL number. The results prove the stability, high solution and the non-oscillation of the scheme. The figures also express that the modified scheme can be efficiently used with time steps as small as required by the CFL stability restriction.

In summary, we have proposed a modified third-order central-upwind scheme and tested two numerical experiments in 2D. In this new scheme, we provide a simpler non-linear limiter of the reconstruction for the two-dimensional Kurganov method and it can satisfy the restrict: $0 \leqslant \theta \leqslant 1$ all the time. The corresponding reconstruction for the modified limiter also keeps non-oscillatory property and high accuracy. The modified scheme simplifies the original flux calculation, unifies the reconstruction functions in the axis directions and the diagonal directions and reduces the computational time consuming. Thus these corrections may be viewed as an extension of the Kurganov scheme. The numerical tests for interaction between a magnetosonic shock and a denser cloud and magnetic reconnection problems prove that the modified scheme is robust and yields reliable results for MHD and RMHD problems. Consequently, this modified central-upwind formulation can be applied to other problems of solar wind simulation, solar disturbances in solar-terrestrial space and interplanetary systems.[25–29]

## References


[1] Kurganov A, Petrova G 2001 *Numer. Math.* **88** 683
[2] Kurganov A, Noelle S and Petrova G 2001 *SIAM J. Sci. Comput.* **23** 707
[3] Kurganov A, Tadmor E 2000 *J. Comput. Phys.* **60** 241
[4] Kurganov A, Tadmor E 2000 *J. Comput. Phys.* **160** 720
[5] Kurganov A, Levy D 2000 *SIAM J. Sci. Comput.* **22** 1461
[6] Bryson S, Levy D 2003 *J. Comput. Phys.* **189** 63
[7] Bryson S, Levy D 2006 *J. Sci. Comput.* **27** 163
[8] Abreu E, Pereira F, Ribeiro S 2009 *Comput. Appl. Math.* **28** 87
[9] Greenshields C J, Weller H G, Gasparini L and Reese J M 2010 *Int. J. Numer. Meth. Fluids.* **63** 1
[10] Dehghan M, Jazlanian R 2010 *J. Vib. Control* (accepted)
[11] Peer A A I, Gopaul A, Dauhoo M Z and Bhuruth M 2008 *Appl. Numer. Math.* **58** 674
[12] Bryson S, Kurganov A, Levy D and Petrova G 2005 *IMA J. Numer. Anal.* **25** 113
[13] Kurganov A, Petrova G and Popov B 2007 *SIAM J. Sci. Comput.* **29** 2381
[14] Kurganov A, Petrova G 2009 *SIAM J. Sci. Comput.* **31** 1742
[15] Harten A, Engquist B, Osher S and Chakravarthy S R 1987 *J. Comput. Phys.* **71** 231
[16] Shu C W 1990 *J. Sci. Comput.* **5** 127
[17] Jiang G S, Shu C W 1996 *J. Comput. Phys.* **126** 202
[18] Liu X D, Osher S and Chan T 1994 *J. Comput. Phys.* **115** 200
[19] Levy D, Puppo G and Russo G 1999 *Math. Model. and Numer. Anal.* **33** 547
[20] Dai W, Woodward P R 1998 *J. Comput. Phys.* **142** 331
[21] Han J Q, Tang H Z 2007 *J. Comput. Phys.* **220** 791
[22] Feng X S, Zhou Y F and Hu Y Q 2006 *Chin. J. Space Sci.* **26** 1
[23] Wei F S, Hu Q and Feng X S 2001 *Chin. Sci. Bull.* **46** 111
[24] Wei F S, Hu Q, Schwen R and Feng X S 2000 *Sci. Chin.* A **43** 629
[25] Xiong M, Peng Z, Hu Y Q, Zheng H N 2009 *Chin. Phys. Lett.* **26** 015202
[26] Zheng H N, Zhang Y Y and Wang S et al 2006 *Chin. Phys. Lett.* **23** 399
[27] Feng X S, Yang L P and Xiang C Q et al 2010 *Astrophys. J.* **723** 300
[28] Feng X S, Hu Y Q and Wei F S 2006 *Sol. Phys.* **235** 235
[29] Hu Y Q, Feng X S 2006 *Sol. Phys.* **238** 329